

Application of density estimation methods to quantal analysis

Koichi Yoshioka

Tokyo Medical and Dental University

Summary

There has been controversy for the quantal nature of neurotransmission of mammalian central synapses. If quantal variance is low, an amplitude histogram of synaptic responses is expected to show equally spaced peaks. However, histograms have disadvantages of being discontinuous and their profile depends on the choice of bin size. In order to obtain a continuous and smooth estimate of probability distribution, we used nonparametric methods of density estimation based on local likelihood or penalized likelihood principle. Application of these methods to GABAergic IPSCs in Purkinje cells in rat cerebellar slices gave smooth but multimodal density estimates of amplitude fluctuations. Analysis of the density curves allowed us to estimate the quantal size. These procedures were used to examine the site of action of amines that induced a long-term facilitation of the IPSCs.

1. Introduction

Plasticity of synaptic transmission is thought to underlie higher functions of brain such as learning and memory. We have been studying the mechanisms of GABAergic transmission in the cerebellar cortex. Inhibitory postsynaptic currents (IPSCs) are recorded either from Purkinje cells or from basket cells using slice patch recording techniques. These GABAergic transmissions are known to be modulated by a number of agents, such as β -adrenergic agonists, serotonin or glutamate. We have been studying the mechanisms of actions of these agents and are particularly interested to know whether their actions are presynaptic or postsynaptic. One of the methods of analyzing changes in synaptic transmission is quantal analysis (Redman, 1990; Stricker and Redman, 1994).

The quantal hypothesis for synaptic transmission assumes that neurotransmitter is released stochastically from the presynaptic terminal in packets (quanta) of similar size. Although the evidence for the quantal release is convincing at the neuromuscular junction, it is much less clear for mammalian central synapses, particularly for inhibitory synapses. A conventional method for analyzing synaptic fluctuations is to construct a frequency histogram of recorded synaptic amplitudes. However, such a histogram is discontinuous

and the profile depends on the choice of bin size. It is therefore desirable to obtain a continuous and smooth estimate of the probability density of the fluctuations. To this end, we applied two methods of density estimation to quantal analysis: local likelihood density estimation (Loader, 1996) and penalized likelihood density estimation (Silverman, 1982).

2. Sample records

In Figure 1A, sample records from a Purkinje cell are shown. IPSCs were evoked by field stimulation at 1 Hz and thirty successive traces are superimposed. To perform quantal analysis, it is desirable to make the signal-to-noise ratio as large as possible. For this purpose, 5 μ M CNQX was added to the perfusion medium to block EPSCs. A recording pipette filled with 140 mM KCl was used, so that the equilibrium potential of the IPSC is about 0 mV and the membrane potential was held at -80 mV. In these conditions the direction of the current is inward and the amplitudes are quite large. In this example, the magnitudes of the current clearly vary in a step-wise manner and the frequency histogram of the amplitude shows discrete peaks, apparently showing quantal nature of synaptic transmission (Fig. 1B).

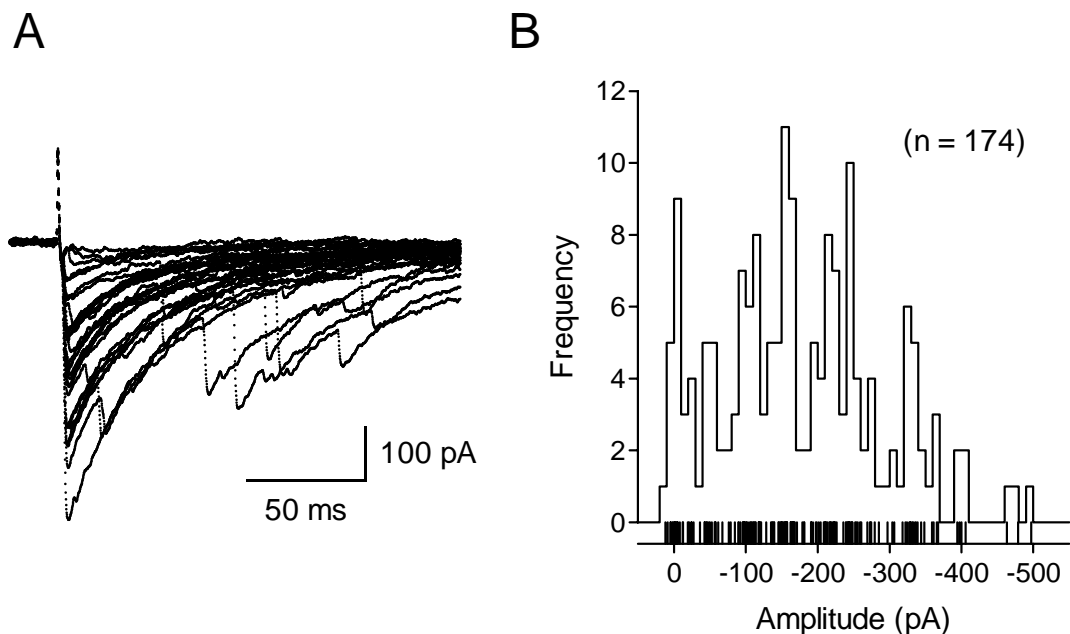


Figure 1. Sample records (A) and histogram (B) of GABAergic IPSCs recorded from a Purkinje cell

3. Parametric quantal models

The classical model of quantal synaptic transmission assumes that the mean amplitudes of quantal components are separated by equal increments (the quantal amplitude) and the variances associated with the components also increment by the variances of quantal components and background noise. The mean of r th quantal component is then given by $\mu_r = rq$, where q is the mean of quantal amplitude and the variance of μ_r is given by $\sigma_r^2 = \sigma_n^2 + r\sigma_q^2$, where σ_n^2 is the noise variance and σ_q^2 is the quantal variance. Assuming that the release process of quanta is described by the binomial or Poisson distribution and that the distributions of each quantal response and noise obey normal distributions, the probability density of amplitude fluctuations is given as a mixture of normal distributions

$$f(x) = \sum_{r=0}^R \pi_r \frac{1}{2\pi(\sigma_n^2 + r\sigma_q^2)} \exp\left[-\frac{(x - rq)^2}{2(\sigma_n^2 + r\sigma_q^2)}\right]$$

where π_r is the binomial or Poisson probability.

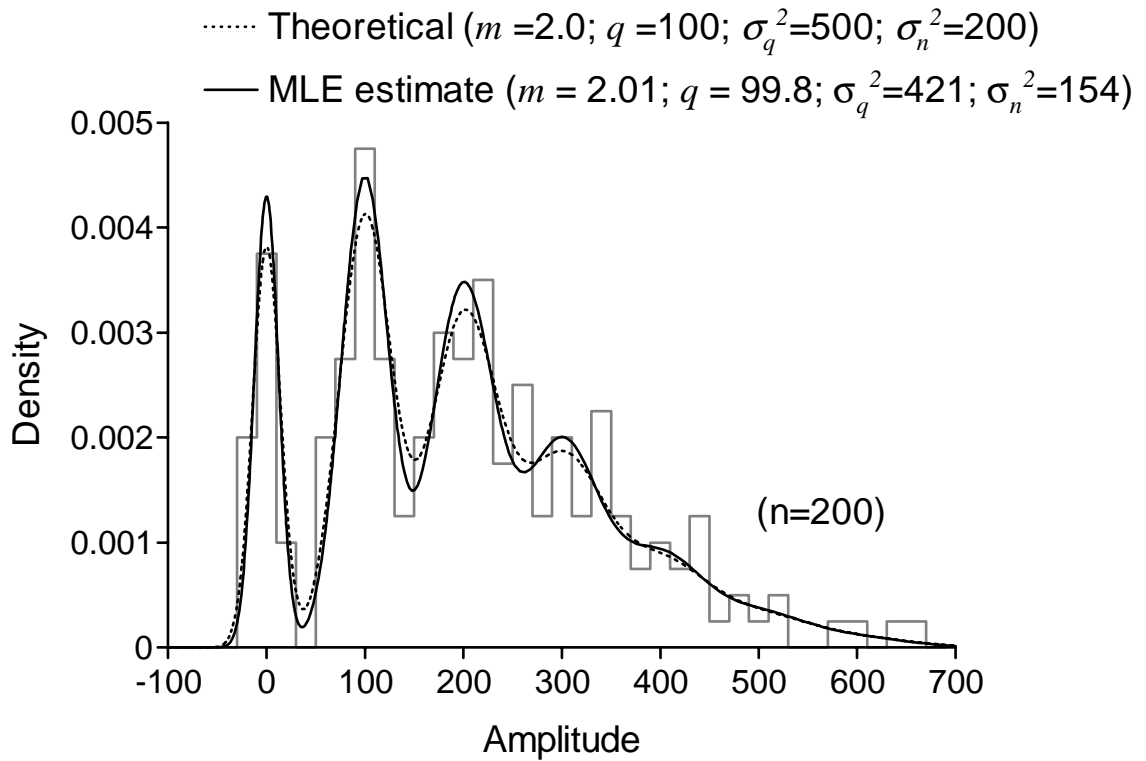


Figure 2. Maximum likelihood fit of the Poisson quantal model to a simulated data set.

Figure 2 illustrates the procedures of estimating quantal parameters of an artificial set of data created by generating random numbers according to the Poisson model. The solid curve is the estimate using the maximum likelihood method. With this method we can obtain estimates of quantal parameters. We applied this approach to the data of IPSCs and found that some of the data could be fitted well by the Poisson or binomial quantal model, but many of the data could not. We therefore turned to nonparametric approach.

4. Density estimation methods

Several types of nonparametric density methods have been proposed. The histogram can be regarded as a simple method of density estimation, but it has several problems: it is a step-wise function and is not smooth; the form of the histogram depends on the choice of the binwidth and also on the choice of the starting point of the histogram (Simonoff, 1996). Using histograms, therefore, it is very difficult to precisely distinguish and locate the peaks in the density.

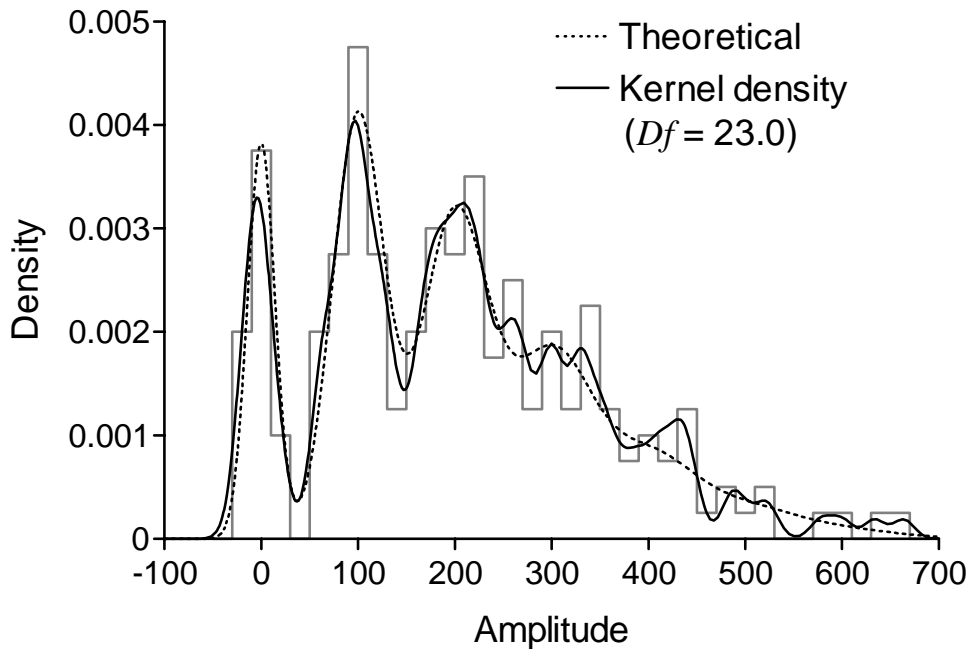


Figure 3. Kernel density estimate to the simulated data set of Figure 2. *Df*: degrees of freedom.

The kernel density is a popular estimator of density. Figure 3 gives the result of applying the kernel density to the same data set of the Poisson model in Figure 2. Smoothness of the estimate depends on the value of the bandwidth h . In this example, the bandwidth was determined by AIC (see below). The peak of failures and the first two quantal peaks are well reproduced, but the curve becomes undulant at peaks of larger amplitudes. The kernel density is known to have some problems, including that it has a boundary bias and its local adaptivity is not sufficient (Simonoff, 1996).

Loader (1996; 1999) recently proposed the local likelihood density estimation. In this method, the likelihood problem with a kernel function K as a weight, is evaluated at each value of x . At x and near x , the logarithm of the density is represented by a polynomial function and the value of the density f at x is given by the exponential of the constant term:

$$L_x(\boldsymbol{\theta}) = \sum_{i=1}^n K\left(\frac{x_i - x}{h}\right) \log f_x(x_i, \boldsymbol{\theta}) - n \int K\left(\frac{u - x}{h}\right) f_x(u, \boldsymbol{\theta}) du$$

$$\log f_x(u, \boldsymbol{\theta}) = \theta_0 + \theta_1(u - x) + \dots + \theta_p(u - x)^p$$

$$\hat{f}(x) = f_x(x, \hat{\boldsymbol{\theta}}) = \exp(\hat{\theta}_0)$$

If only the constant term is used for the polynomial, the estimate reduces to the kernel density. Using a higher polynomial is expected to reduce the bias of the kernel estimator and to show more local adaptivity. Usually, the polynomial degrees of one or two, that is, local linear or quadratic function, are sufficient (Loader, 1996; 1999).

The method also contains the bandwidth h as a smoothing parameter, which can be determined by AIC with the following formula (Loader, 1999).

$$\text{AIC}(\hat{f}) = -2 \sum_{i=1}^n \log \hat{f}(x_i) + 2 \sum_{i=1}^n \text{infl}(x_i) + 2n \left(\int \hat{f}(u) du - 1 \right)$$

$$\mathbf{H}(x) = -\frac{\partial^2 L_x}{\partial \boldsymbol{\theta} \partial \boldsymbol{\theta}^T}$$

$$\text{infl}(x) = K(0)(\mathbf{H}^{-1})_{11}(x)$$

$$\nu = \sum_{i=1}^n \text{infl}(x_i)$$

where ν is called the degrees of freedom.

The solid curve in Figure 4 is the local quadratic estimate of the Poisson model data with the bandwidth determined by AIC. The quantal peaks of larger amplitudes are smoother and more faithfully estimated than the kernel density method. This kind of simulation suggested appropriateness of this method for application to quantal analysis. However, when we estimate the densities of actual data, it will be desirable to have another method of different principle, and if the two different methods give similar results, we will be more convinced with the results.

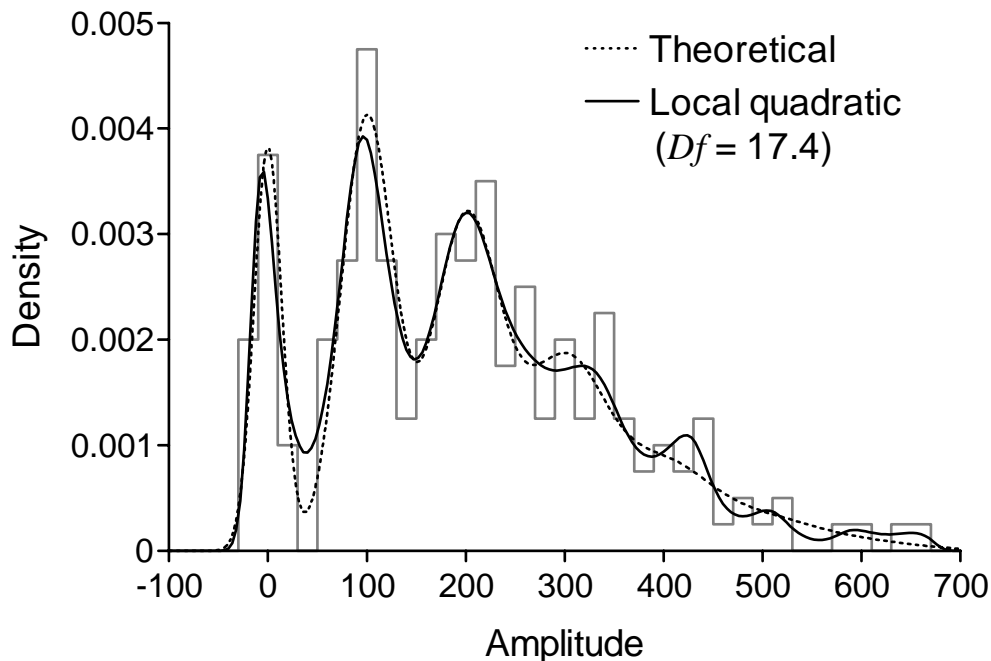


Figure 4. Local quadratic estimate to the simulated data set.

We therefore tried another method of density estimation: penalized likelihood method of Silverman (1982). This method is again an extension of the maximum likelihood principle, but the idea is different from the local likelihood. As in ordinary maximum likelihood methods, it is a global likelihood principle, but it contains an additional term called roughness penalty. This penalty term ensures the smoothness of the estimator and the degree of smoothness is controlled by the smoothing parameter λ . In actual calculation, the logarithm of density is represented by a spline function. And the smoothing parameter λ again can be determined by AIC (O'Sullivan, 1988).

$$L(f) = \sum_{i=1}^n \log f(x_i) - \Phi - n \int f(u) du$$

$$\Phi = \frac{n\lambda}{2} \int [D^m(\log f)(u)]^2 du$$

$$\log f(x) = \sum_{i=1}^M \alpha_i B_i(x)$$

$$\text{AIC}(\hat{f}) = -2 \sum_{i=1}^n \log \hat{f}(x_i) + 2 \text{tr}([\hat{\mathbf{J}} + \lambda \mathbf{K}]^{-1} \hat{\mathbf{J}})$$

$$\hat{\mathbf{J}}_{ij} = \int \exp[\sum_{i=1}^n \hat{\alpha}_i B_i(u)] B_i(u) B_j(u) du, \quad \mathbf{K}_{ij} = \int B^{(m)}_i(u) B^{(m)}_j(u) du$$

where the trace term in the AIC formula corresponds to the degrees of freedom.

Figure 5 shows the penalized likelihood estimate of the Poisson model data with λ determined by AIC. The derivative of penalty of order 3 is used in this calculation. The estimated curve is very smooth and quantal peaks are satisfactorily estimated.

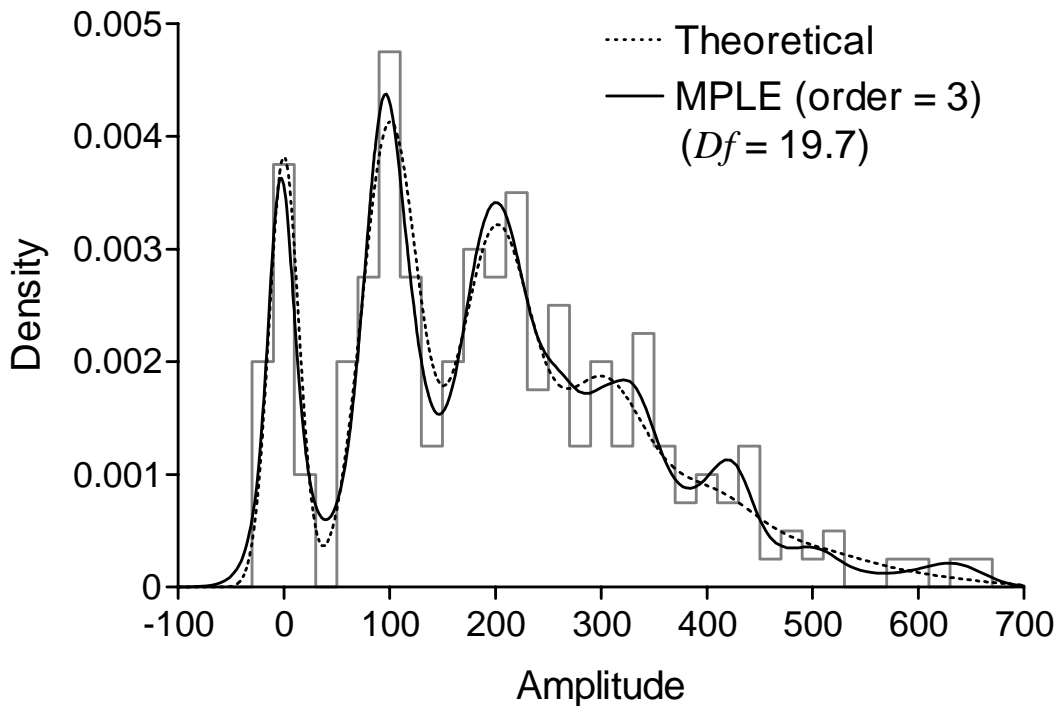


Figure 5. Maximum penalized likelihood estimate (MPLE) of order 3 to the simulated data set.

5. Estimation of quantal amplitude

Figure 6A shows a superimposition of the local likelihood and penalized likelihood estimates to the simulated data set. They are very close to each other and close to the theoretical curve. When the quantal peaks are equally separated as in this case, the quantal size can be estimated as the period of the peaks. To this end, we can take the spectral density function of the density curve using Burg's method, as shown in Fig. 6B. The spectrum has a large DC component, which corresponds to the overall trend of the density, and a single peak at 0.01 of the frequency. The reciprocal of the frequency gives an estimate of the period, 100 in this case, which exactly coincides with the quantal size of the model we used.

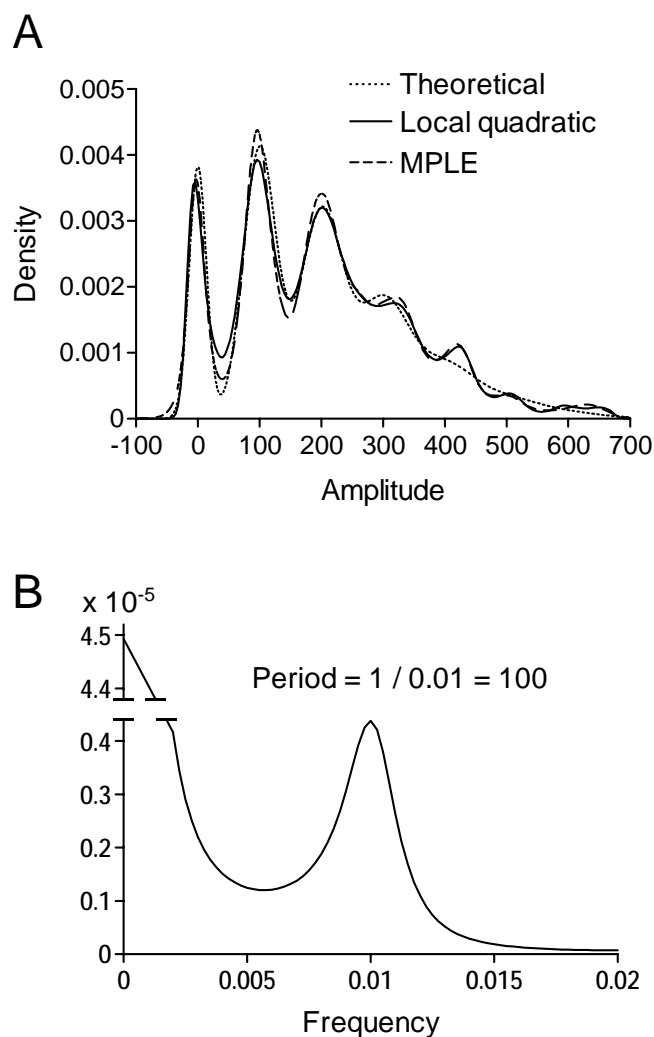


Figure 6. A. Superimposition of local likelihood and penalized likelihood estimates to the simulated data set. B. Spectral density estimate for the penalized likelihood estimate.

6. Application of density estimation methods to IPSC data

Figure 7A gives the local likelihood density estimate of the sample data set of IPSCs shown in Figure 1. Very clear and smooth peaks are observed and the first several peaks are almost equally spaced. The lower panel shows the penalized likelihood estimate of the same data. The estimated curve is quite similar to the local likelihood estimate.

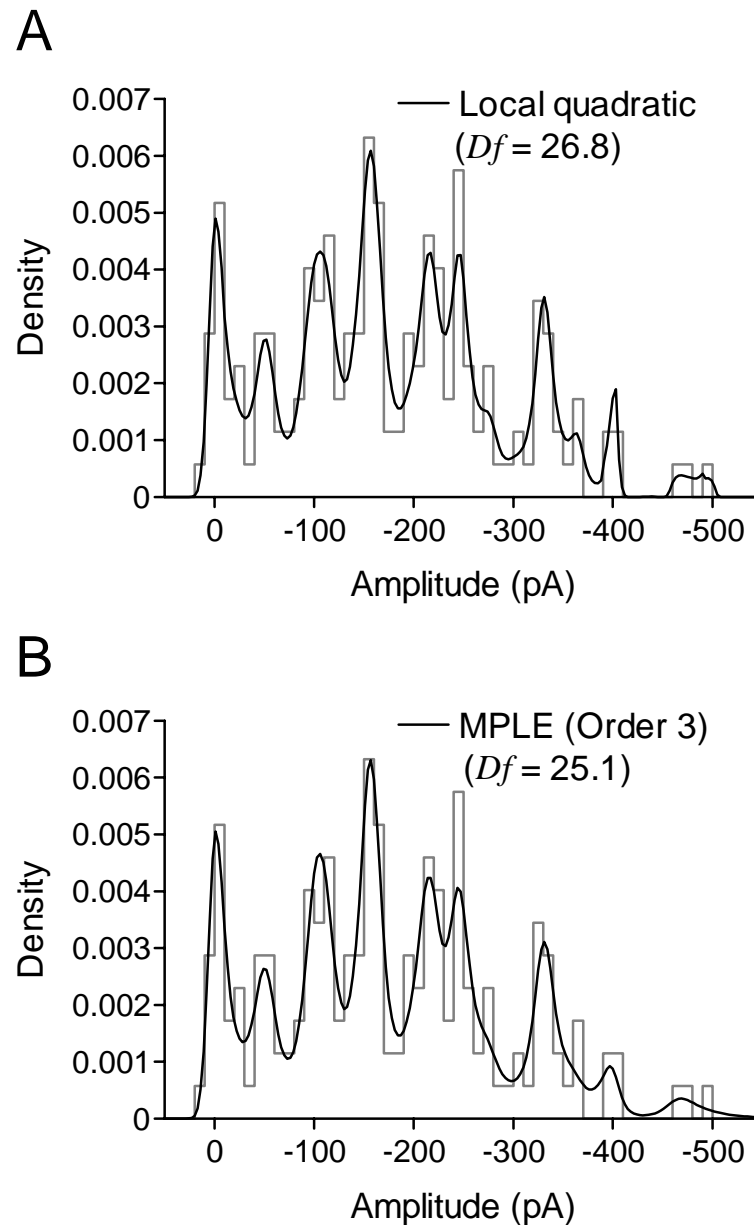


Figure 7. Local likelihood (A) and penalized likelihood (B) estimates to the data of IPSCs shown in Fig. 1.

Figure 8 gives a superimposition of the two estimates, showing that the two curves are almost identical, except for larger values of amplitude. The lower graph is the spectral density of the penalized likelihood estimate. It has a single sharp peak and the period is estimated to be 53.3 pA. The vertical lines in the upper graph are drawn with a constant interval of this value starting at 0 pA. In addition to the peak of failures, the first four non-zero peaks are located almost exactly on these lines. This strongly suggests that they are in deed quantal peaks with the quantal size being about 53 pA.

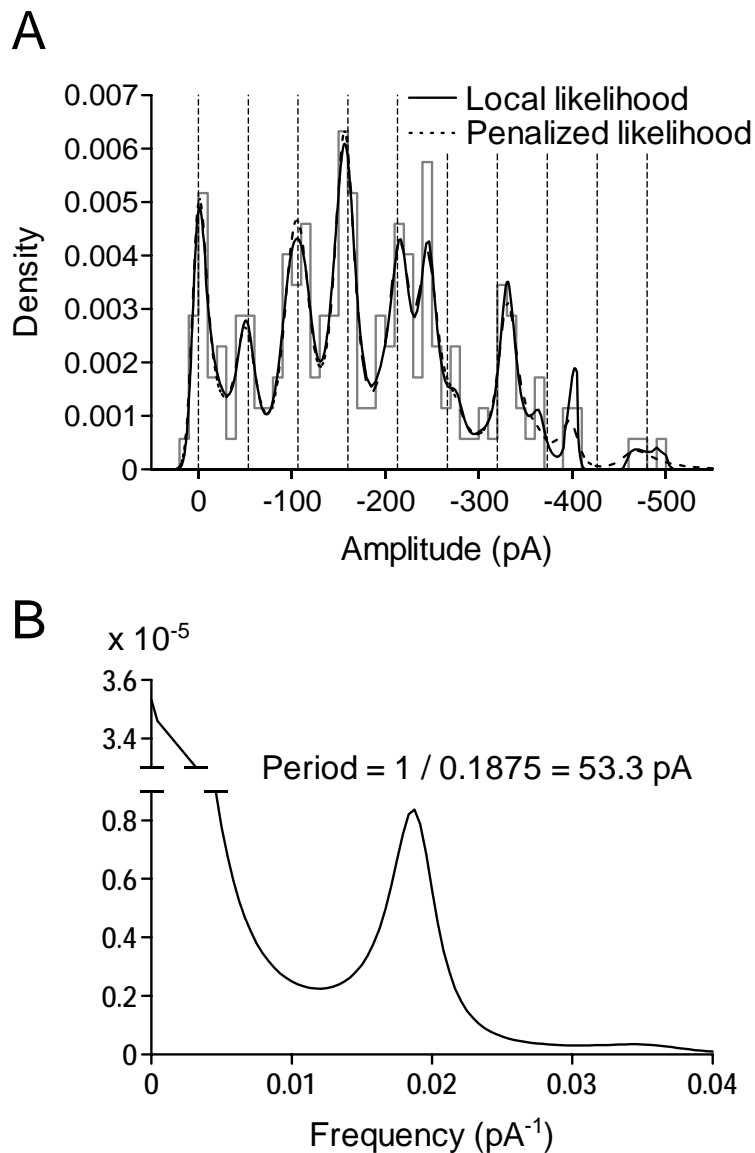


Figure 8. A. Superimposition of local likelihood and penalized likelihood estimates shown in Fig. 7. B. Spectral density estimate for the penalized likelihood estimate.

7. Effect of voltage changes

In Figure 9, the effect of changing the holding potential is shown. Changing the holding potential from -60 mV to -80 mV makes the driving force larger and thus the responses become larger. In this manipulation, we expect that the positions of quantal peaks are expanded proportionally, but other statistics of the responses should remain the same. As expected, the proportions of failures are the same in both cases. When the current scale of the density estimate at -60 mV is increased by 125% and superimposed on the estimate of -80 mV, the positions of the first four peaks are almost the same and the areas under the components are quite similar. This type of change may be regarded as a result of a postsynaptic effect.

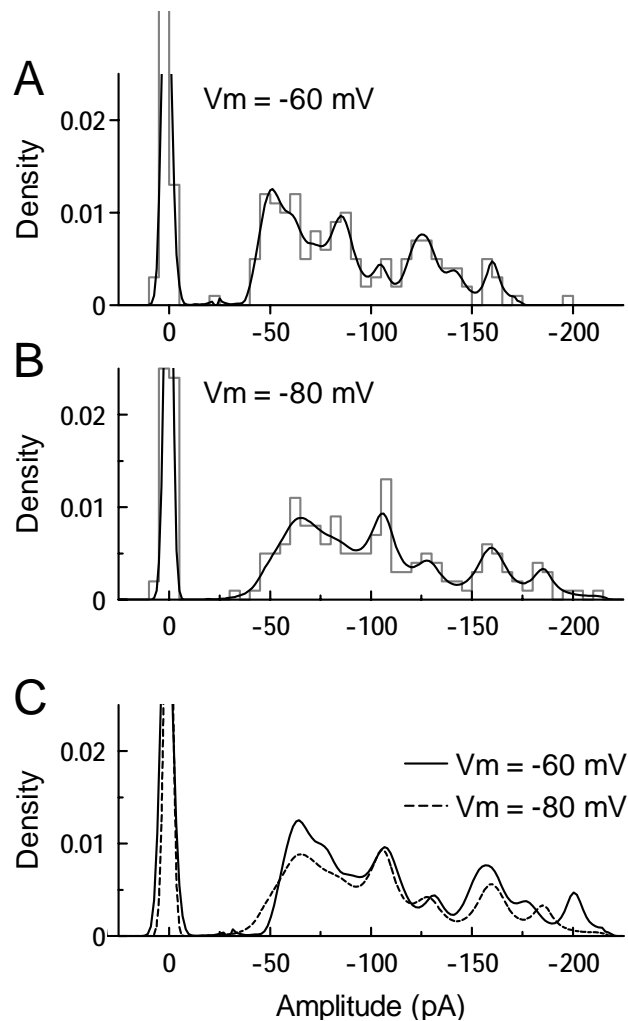


Figure 9. Effect of changing the holding potential on the amplitude distributions

8. Effect of Ca concentrations

Figure 10 illustrates the effect of lowering Ca and increasing Mg concentrations on the amplitude distributions. By this manipulation, the proportion of failures is increased by about 3-fold, and the peaks of large amplitudes disappeared. In Fig. 10C, the two estimates are superimposed with the same abscissa and ordinate scales. It appears that there is one-to-one correspondence between the first three peaks. This kind of changes may be a typical of a presynaptic effect.

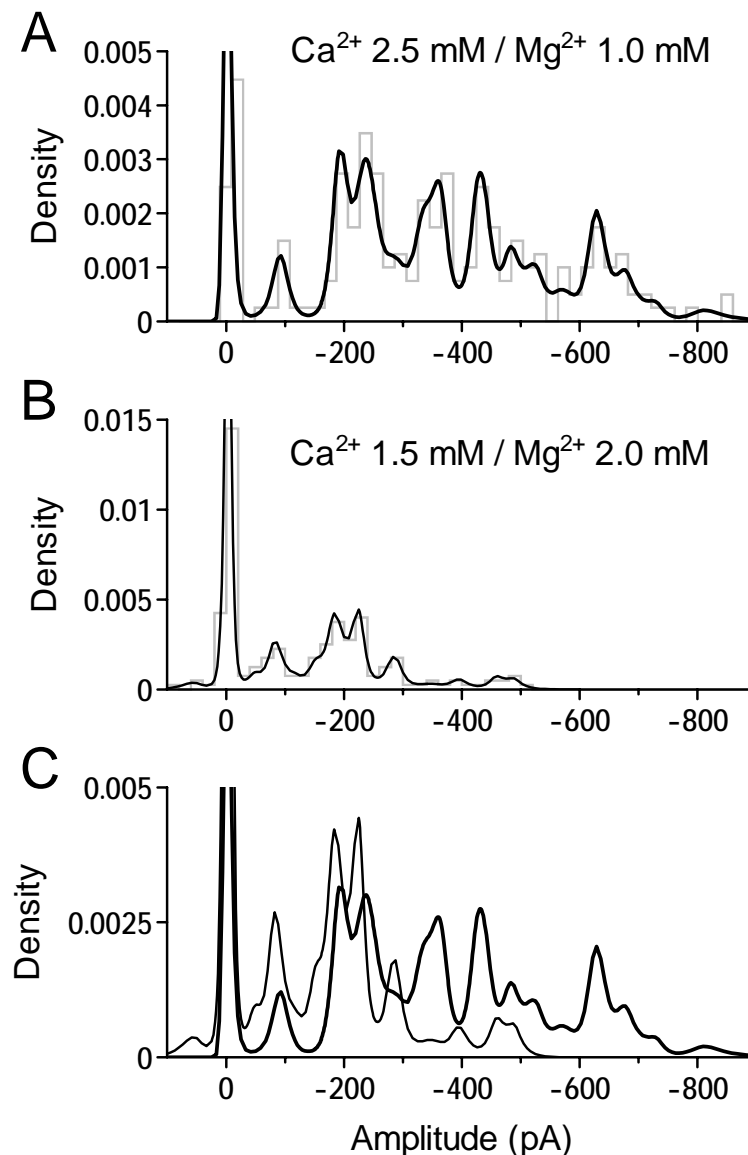


Figure 10. Effect of lowering Ca and increasing Mg concentrations on the amplitude distributions.

9. Effect of isoproterenol

Mitoma and Konishi (1999) recently showed that β -receptor activation causes a facilitation of GABAergic IPSCs in the rat cerebellar cortex. Figure 11A shows the density estimate in the control condition. Again several peaks can be observed in the density estimate. Figure 11B and C show the effect of the β -agonist, isoproterenol (Isp) in two different periods after introduction of Isp. In the first period after applying Isp, it can be seen that the proportion of failures is decreased and in stead the proportion of the first non-zero peak is increased. In the later period, the height of the first peak is decreased and the third peak is increased.

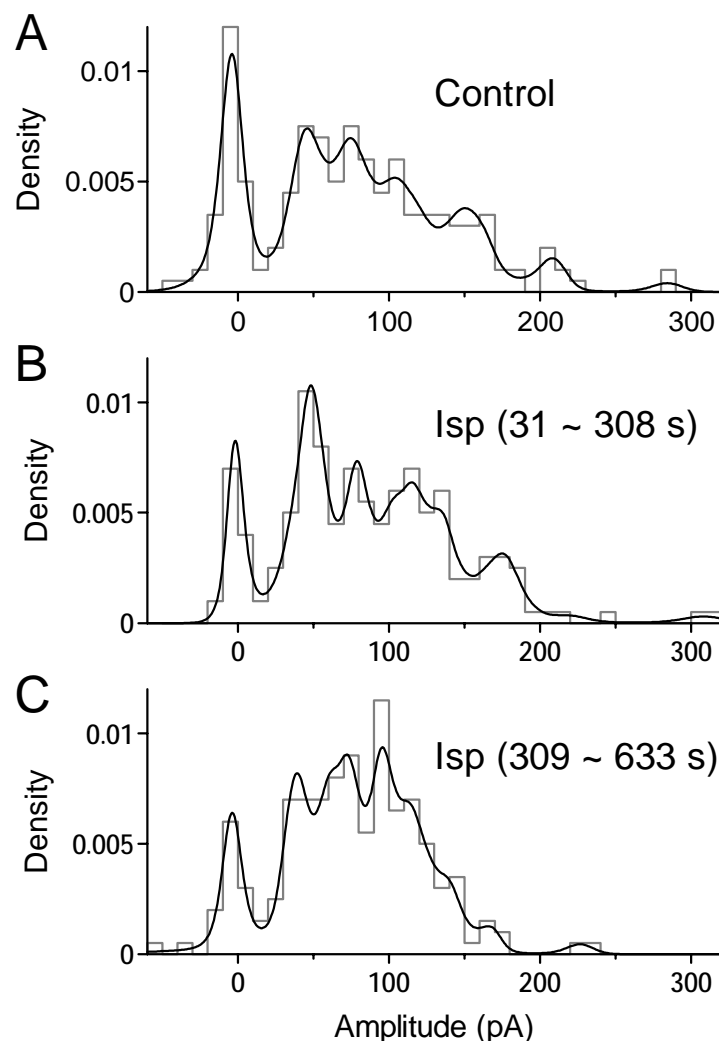


Figure 11. Effect of isoproterenol on the amplitude distributions.

In Figure 12, the three curves are superimposed. The first three peaks are presumably corresponding and the effect of Isp is to decrease the proportion of failures and increase the peaks of larger amplitudes. In this case, there may be a slight sign of left-ward shift in the positions of these peaks in the later period of Isp treatment. This experiment suggests that the potentiating effect of Isp is not due to an increase in the quantal amplitudes but due to a change in the statistics of the response.

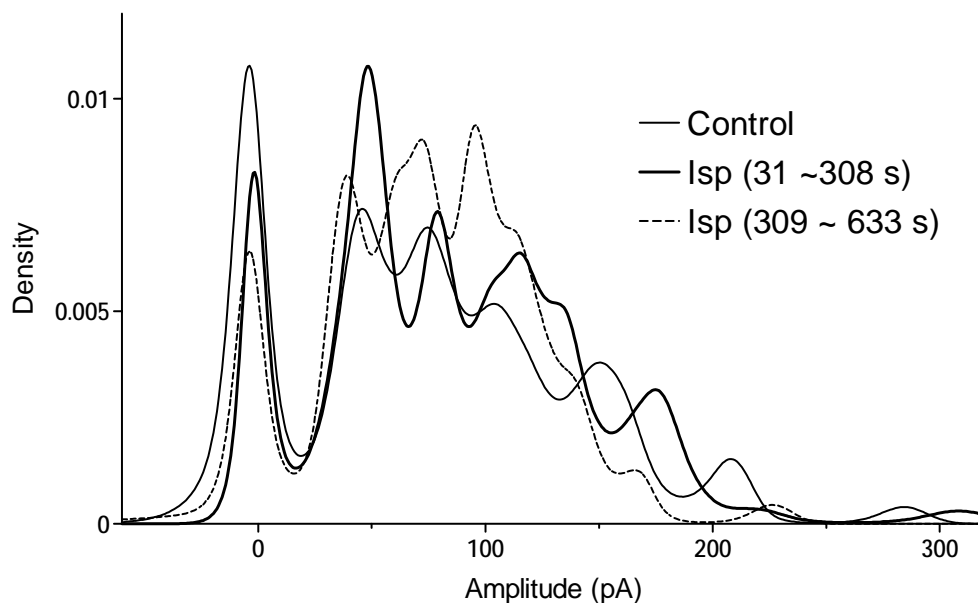


Figure 12 Superimposition of the three density estimates in Figure 11.

10. Conclusion

Application of nonparametric density estimation methods revealed discrete peaks in the amplitude distribution. When the peaks were equally separated, an estimate of the quantal size could be obtained. When the synaptic transmission was modulated by some manipulations, we could obtain information about the mechanisms of the changes by tracing the changes in peak components in the density estimates.

References

1. Simonoff, J.S. Smoothing Methods in Statistics. Springer, New York, 1996.
2. Loader, C.R. Local Regression and Likelihood. Springer, New York, 1999.
3. Silverman, B.W. On the estimation of a probability density function by the maximum penalized likelihood method. *Ann. Statist.* 10: 795-810, 1982.
4. O'Sullivan, F. Fast computation of fully automated log-density and log-hazard estimators. *SIAM J. Sci. Statist. Comp.* 9: 363-379, 1988.
5. Loader, C.R. Local likelihood density estimation. *Ann. Statist.* 24: 1602-1618, 1996.
6. Redman, S. Quantal analysis of synaptic potentials in neurons of the central nervous system. *Physiol. Rev.* 70: 165-198, 1990.
7. Stricker, C. and Redman, S. Statistical models of synaptic transmission evaluated using the expectation-maximization algorithm. *Biophys. J.* 67: 656-670, 1994.
8. Mitoma H, Konishi S. Monoaminergic long-term facilitation of GABA-mediated inhibitory transmission at cerebellar synapses. *Neuroscience.* 88: 871-83, 1999.